Sveriges lantbruksuniversitet
Swedish University of Agricultural Sciences

Faculty of Natural Resources and Agricultural Sciences

Catchment influences on mercury methylation in a peatland chronosequence

Robin Hagblom

Master´s thesis • 30 credits

Department of Aquatic Sciences and Assessment
Uppsala 2018

Catchment influences on mercury methylation in a peatland chronosequence

Robin Hagblom

Supervisor:	Baolin Wang, Swedish University of Agricultural Sciences, Department of Aquatic Sciences and Assessment
Examiner:	Dan Berggren Kleja, Swedish University of Agricultural Sciences, Department of Soil and Environment

Credits:	30 credits
Level:	Second cycle, A2E
Course title:	Independent project/degree project in Soil Science - Master´s thesis
Course code:	EX0430
Place of publication:	Uppsala
Year of publication:	2018
Online publication:	https://stud.epsilon.slu.se
Keywords:	Methyl Mercury, GIS, Northern Peatland, Mire, Water-shed, Elevation

Swedish University of Agricultural Sciences
Faculty of Natural Resources and Agricultural Sciences
Department of Aquatic Sciences and Assessment

Catchment Influences on mercury methylation in a peatland chronosequence

Robin Hagblom

Abstract

Since the beginning of industrialization, emissions of mercury (Hg) from human activities in excess of natural levels have increased deposition rates to ecosystems, storage in soils and loading to aquatic environments. Toxicity to animals, subject to this accumulation, as well as to humans consuming them, are the major concerns driving research on this subject. Peatlands play a key role in Hg cycling as hotspots for Hg methylation, methyl mercury (MeHg) being a particularly mobile, bioavailable form of Hg that is prone to bioaccumulation. Underlying geography is fundamental in shaping the hydrology of a given area and, therefore, the locations of points of accumulation and methylation of Hg.

In this study, potential relationships between geographic parameters, elucidated via GIS analysis were investigated with the aim of identifying which parameters were relevant as explanatory variables in the prediction of Hg concentrations in the study area. Elevation was expected to strongly predict MeHg concentrations due to the presence of a local chronosequence, created by land rise. The land's age since emergence from the sea ranges from years to thousands of years within a span of 10 km, enabled this investigation in an environment in which climate is controlled for.

With 13 of the 15 watershed areas less than 1 ha and 9 less than 500m^2, little of meaning could be concluded from statistical analysis with certainty. Linear regression and PLS pointed to Elevation's relationship with THg, PLS implicated Watershed Area as being associated with MeHg, and PCA hinted at the relevance of Area as well as a cluster of Slope, Downslope Index, Curvature, and % Forest for sample sites with extreme values of Hg and other metals. Our results indicate that elevation alone is not a strong predictor of MeHg concentration along this peatland chronosequence.

Keywords: Methyl Mercury, GIS, Northern Peatland, Mire, Watershed, Elevation

Popular Summary

Industrialization has led to large emissions of mercury from human activities to the atmosphere. Mercury can travel long distances in the atmosphere before it is deposited to land, where it tends to accumulate in soil, vegetation, and wildlife, which poses a threat to the environment and humans.

Virtually all soils are home to bacterial communities. In soils that are saturated with water, anaerobic bacterial communities dominate and some of these are able to convert the mercury that is deposited from the atmosphere into a form called methyl mercury in a process called mercury methylation. Methyl Mercury is considered the most dangerous form of mercury because it is both toxic and tends to accumulate in animals, such as fish, more than other forms.

Peatlands are a type of soil that is usually saturated with water, which makes these soils common sites of mercury methylation. Peatlands are also common in northern Sweden where mercury deposition has been high despite relatively little release of mercury, again because mercury can travel long distances in the atmosphere.

Water that feeds into peatlands can travel over and through soils and take with it mercury along the way. Mercury that is thinly deposited to a large area, therefore can be concentrated in peatlands where methyl mercury can be created at high levels. Once methyl mercury has been created it can be transported further downstream to waterbodies where it can accumulate in fish that humans might eat.

How water moves across a landscape, through peatlands to downstream waterbodies is defined by the geography. This study area was special because of the presence of a chronosequence created by land rise where, over a short distance, the time since the emergence of land from the Baltic Sea is proportional to elevation. The younger and lower the land, the more nutrients in the soil, which should lead to more mercury methylation. The chronosequence meant peatlands with different ages and nutrient levels could be studied all in the same climate and background environment.

In this study, the relationships between geography and mercury concentrations at 15 sample peatlands were investigated to see if the geography itself could explain what the mercury concentrations were at the different peatland sample sites.

Because age, elevation. and nutrient status were so closely related, it was first thought that elevation could explain most of the differences in mercury concentration at the different study sites. But the relationships were not that simple. Watershed area (the area of land from which water feeds into a peat-

land) for each peatland was then looked at along with other geographic parameters, including how much of the watershed was made up of peatland or forest. Though no relationships were strong enough to fully explain why mercury concentrations were what they were, watershed area was clearly an important factor and how much peatland vs. forest might be as well.

Table of contents

Abbreviations

Hg	Mercury
Hg(0)	Elemental Mercury
Hg(II)	Divalent Mercury Cation
THg	Total Mercury
MeHg	Methyl Mercury Cation
MeHg:THg	Methyl Mercury to Total Mercury ratio
SOM	Soil Organic Matter
SRB	Sulfate-Reducing Bacteria
IRB	Iron-Reducing Bacteria
VIP	Variable Importance Projection

1 Introduction

Since the beginning of industrialization, emissions of mercury (Hg) from human activities in excess of natural levels have increased deposition rates to ecosystems, storage in soils and loading to aquatic environments (Lindberg et al., 2007; Swartzendruber and Jaffe, 2012; UNEP, 2013). Soils often act as a buffer by retaining much of the deposited Hg but significantly elevated levels can still be present in downstream aquatic ecosystems where Hg can accumulate as it climbs trophic levels (Morel, Kraepiel and Amyot, 1999). Toxicity to animals, subject to this accumulation, as well as to humans consuming them, are the major concerns driving research on this subject (Amirbahman and Fernandez, 2012). Peatlands play a key role in Hg cycling as hotspots for Hg methylation, methyl mercury being a particularly mobile, bioavailable form of Hg that is prone to bioaccumulation (Grigal, 2003; Shanley and Bishop, 2012).

Atmospheric deposition of Hg represents the main input of Hg into forested watersheds, which often contain peatlands, even affecting relatively pristine northern ecosystems (Figure 1) (Lindqvist et al., 1991; Iverfeldt 1991; Mason, Fitzgerald and Morel, 1994; Grigal 2003). While high latitude peatlands constitute approximately 3.4% of global land area (Kivinen and Pakarinen, 81), 15% of Sweden's surface is covered by peatlands, making the risk of dangerously high levels of MeHg produced in peatlands and transported to downstream water bodies of particular concern in Sweden (Rudd, 1995; Schoning, Sohlenius and Mikko, 2012).

The dominant forms of Hg in atmospheric deposition are elemental mercury (Hg(0)), as a gas or dissolved in wet deposition (Slemr, Schuster, and Seiler, 1985); and divalent mercury (Hg(II)), dissolved, associated with particulate matter (HgP), or as reactive gaseous mercury (RGM) (Ross and Vermette, 1995; Lindberg and Stratton, 1998). Gaseous elemental mercury (GEM) is the most abundant form of mercury in the atmosphere (Slemr, Schuster, and Seiler, 1985). Its relative stability in the atmosphere, in part due to its low solubility in water, leads to a longer residence time than Hg(II) (years vs. weeks) and enables atmospheric transport on a hemispheric scale (Lin and Pehkonen, 1999); Hg(II) tends to be deposited closer to

its source of emission (Lindberg and Stratton, 1998). Conversion between these two forms occurs in the atmosphere through redox reactions often extending residence times (Holmes et al., 2010).

Terrestrial components of a watershed receive the largest proportion of atmospheric Hg input due to the combination of their greater areal extent relative to that of associated water bodies and the expansive surface area provided by the vegetative canopy (St. Louis et al., 2001; Amirbahman and Fernandez, 2012). In forested watersheds, Gaseous Hg(0) tends to enter vegetation through leaf stomata and reach the forest floor via litterfall (Figure 2) (Lindberg et al., 1992). Hg(II) predominantly adsorbs to leaf surfaces and makes up the major fraction of Hg that reaches the forest floor via throughfall (Rea, Lindberg and Keeler, 2001). With respect to means of input, litterfall usually dominates in deciduous forests and throughfall usually dominates in coniferous forests, but due to the volatilization and reemission of large portions of throughfall Hg following reduction from Hg(II) to Hg(0), litterfall is usually the dominant source of Hg that accumulates in soil in both types of forest (Demers et al., 2007).

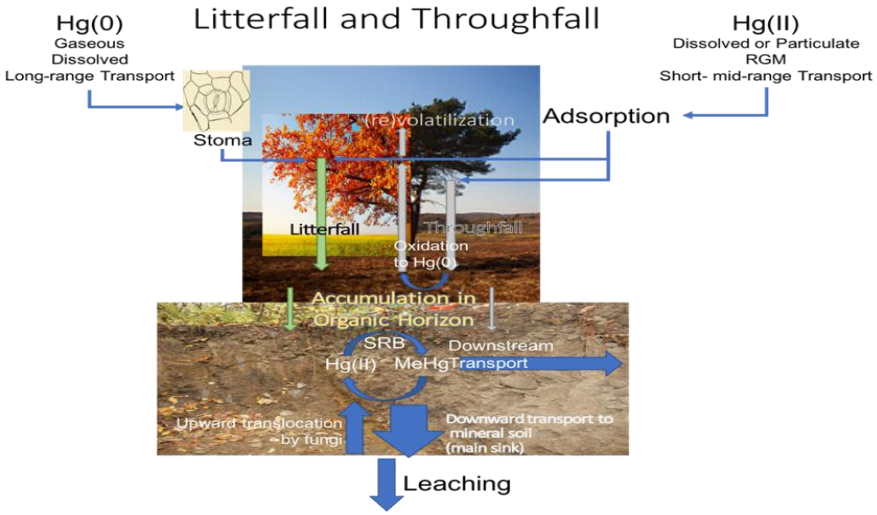

Figure 1. Hg deposition, cycling, and transport in forest and soil. Fluxes are not to scale

The affinity of Hg(II) to bind reduced sulfur species and other functional groups present in soil organic matter (SOM) explains the dependence of Hg storage and transport on organic matter in soils following atmospheric deposition (Xia et al., 1999; Qian et al., 2002). The downward transport of Hg from organic horizons to mineral horizons also follows the movement of SOM (Hissler & Probst, 2006; Amirbahman and Fernandez, 2012). Although soil Hg concentrations tend to be highest in organic horizons (Nater and Grigal, 1992), the main terrestrial Hg pool is the mineral soil due to larger total amounts of SOM and the larger number of available binding sites in the more humified mineral SOM (Grigal, 2003). It is this ability

to store Hg, combined with the tendency of Hg to be transported from forest soils that will make soils a source of so-called “legacy Hg” to downstream aquatic ecosystems into the future despite recent decreases in Hg emissions (Mason, Fitzgerald and Morel, 1994; Bishop et al., 1995; Demers et al., 2013).

Of importance in the study of Hg in nature is the production of monomethylmercury(II) cation (MeHg). While each species state of Hg presents its own forms of toxicity (Guallar et al., 2002; Trasande, Landrigan and Schechter, 2005; Scheuhammer et al., 2007; Bernhoft, 2011), MeHg’s mobility in the environment and tendency to bioaccumulate and biomagnify in food webs has made it a primary focus of Hg ecotoxicology (Fischer et al., 1995; Schlüter, 1996; Patra & Sharma, 2000; Mason, Laporte and Andres, 2000).

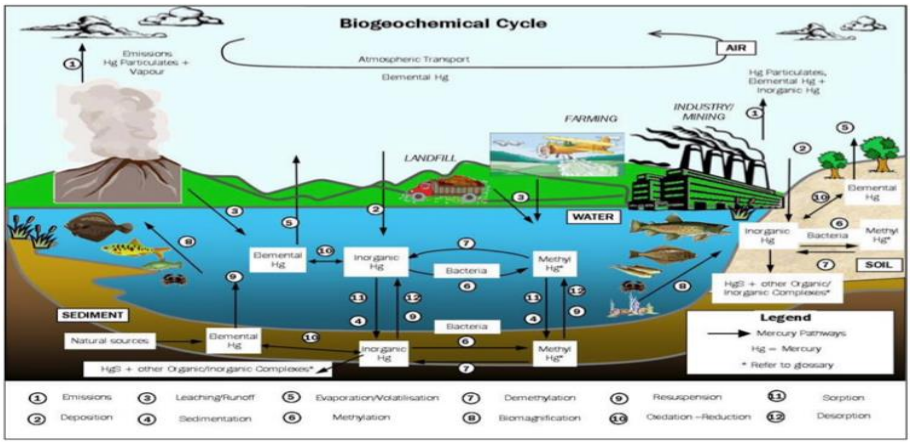

Figure 2. The biogeochemical cycle of Hg (from Chrystall and Rumsby, 2008)

Atmospheric influxes of MeHg to watersheds in deposition are generally negligible (Fitzgerald and Clarkson, 1991; Bishop et al., 1995). It is instead produced within the watershed, mostly by sulfate-reducing bacteria (SRB), which use H_2, organic acid substrates, formate, or short-chain alcohols as electron donors (Compeau and Bartha, 1985; Keller et al., 2014). Iron-reducing bacteria (IRB) have also been shown to methylate mercury but mostly at circumneutral pH, while excessively high Fe concentrations negatively affect methylation rates due to complexation and thus sequestration of Hg and sulfides (Mehrotra and Sedlak, 2005; Fleming et al., 2006; Si et al., 2015). Limiting concentrations of these electron acceptors impede these bacteria and thus mercury methylation (Keller et al., 2014; Fleming et al., 2006).

Abiotic production of MeHg can proceed via certain humic compounds but such production usually represents less than 10% of total production (Nagase et al., 1984, Compeau and Bartha, 1985). Because mercury methylation is carried out by anaerobic soil microorganisms, bioavailability of substrate but also anoxic conditions are essential for this process.

The requirement of suboxic conditions for methylation, then, underlies the status of hydric soils and wetlands as methylation hotspots whereas well-drained soils often play host to the opposite reaction: demethylation (St. Louis et al., 1994; Grigal, 2003). These two processes tend to occur simultaneously in any context, but local conditions define which dominates. For example, in many forest watersheds, upland soils and wetlands act as counterweights regarding Hg methylation (St. Louis et al., 1996). Relative areal extent of such soil types, along with type of wetland, and annual water yield, therefore, often define whether a given catchment is a net source or sink of MeHg (St. Louis et al., 1996). In cases where forest watersheds are sources, the recipients of the wetland-produced MeHg are generally downstream boreal aquatic ecosystems, with MeHg often transported via complexation with DOM or associated with particulate matter dislodged via soil erosion (Rudd, 1995; Bergman et al., 2012). Upon downstream transport, MeHg accumulates in compartments ranging from stream sediment (Schuster et al., 2008) to plankton and microalgae in lakes (Morel, Kraepiel and Amyot, 1999), and up through increasing trophic levels to the fat and muscle tissues of carnivorous birds, mammals, and fish (Driscoll et al., 1994; Morel, Kraepiel and Amyot, 1999; Scheuhammer, 2007).

Beyond the presence of anthropogenic Hg in the environment, human activities may also contribute to the production of MeHg. The digging of ditches and certain forestry practices such as clear cutting have been shown to contribute to increased rates of methylation, largely due to alterations to the local water balance and connectivity (Kronberg et al., 2016). Even attempts to combat other environmental threats such as recreating wetlands to promote biodiversity, and limit eutrophication and flooding may have the unintended effect of creating potential methylation hotspots (EEC, 1992; Morris et al., 2014).

The presence of a chronosequence in the study area, created by land rise and along which the land's age since emergence from the sea ranges from years to thousands of years within a span of 10 km, enabled this investigation in an environment in which climate is controlled for. While age is proportional to elevation, a gradient of nutrient status, assumed to include Sulfur, is also present but inversely proportional to elevation and age. As described above, a Sulfur gradient would be expected to strongly contribute to any explanation of geographic trends in MeHg concentrations.

Underlying geography is fundamental in shaping the hydrology of a given area and, therefore, the locations of points of accumulation and methylation of Hg. In this study, potential relationships between geographic parameters, elucidated via GIS analysis were investigated with the aim of identifying which parameters were relevant as explanatory variables in the prediction of Hg concentrations in the study area.

1.1 Aim

The aim of this report was to investigate possible links between concentrations of Hg and major ions, and a suite of GIS parameters, representing the geography and hydrology of a peatland-rich area in northern Sweden.

1.2 Hypotheses

The primary hypothesis of the chronosequence study, from which data was obtained for this study, was that Elevation at each of 15 sample sites would be able to explain variation in Hg concentrations at the sample sites because of its correlation with age and succession, which in turn shapes the biogeochemistry of peatlands.

A secondary hypothesis was that other characteristics of the catchment (termed GIS parameters in this document) in which peatlands are situated also affect the production of MeHg

2 Materials and Methods

2.1 Study Area, Sampling, and Measurement

Study Area

The study area (63.884971, 20.677078), north (<50 km) of Umeå in northern Sweden, was chosen for its terrestrial ecosystem chronosequences that span ages of ~4000 years within <10 km from the coast, which were created by land rise following the last ice age (Figure 3). Through land rise, nutrient-rich soil constantly emerges from the sea. Previously-emerged soils increase in elevation with continued rise, which is associated with alterations in the availability of electron acceptors (i.e. Sulfate). The small size of the area meant climate and geological setting were relatively uniform and differences in the state and biogeochemistry of the peatlands were expected to be ascribable to differences in watershed hydrogeochemistry and the composition of plant and microbial communities. The rarity of active land rise and the resulting chronosequences combined with the proximity to existing research infrastructure, makes this study area a unique opportunity to study different hypotheses.

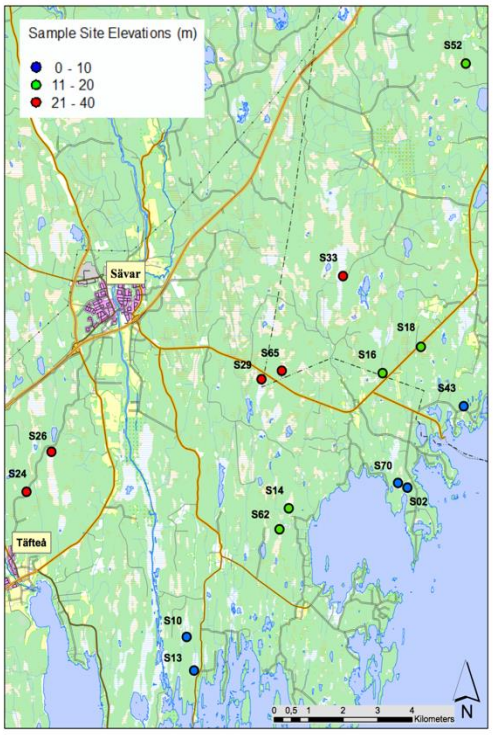

Figure 3. Map of the study area with 15 Sample Sites (colour-coded by elevation, see legend). (Översiktskartan, vector © Lantmäteriet)

Sample Site Selection

Fifteen peatlands, comprising three groupings of five peatlands each, were chosen as sample sites along a chronosequence created by post-glacial rebound. The three groupings represent low (0-10 m, $\lesssim$ 200 years old), mid (11-20 m, ~ 1500 years old) and high (21-40 m, ~ 3500 years old) elevation (and age) with low-elevation sites nearest the Baltic Sea and high-elevation sites farthest inland (Figure 4, Table 1). Of particular importance in this study was the expected presence of a geochemical gradient, including sulfur, along the chronosequence, with high levels in the most recently emerged soils at low elevations, and low levels in the older soils at high elevations.

Table 1. *Sample site locations and elevations*

Sample Site	**N**	**E**	**Elevation (m)**
S02	780736.116	7093002.623	0.9
S70	780463.883	7093132.526	1.5
S43	782371.035	7095258.481	3.3
S13	774557.424	7087933.121	3.5
S10	774341.74	7088864.381	4.8
S52	782428.539	7104754.128	10.1
S14	777301.124	7092427.81	14.1
S16	781128.434	7096903.171	14.6
S18	780017.315	7096175.554	14.6
S62	777031.307	7091847.384	15.6
S29	776508.839	7096007.211	27.2
S26	770421.949	7093995.797	28.9
S33	778871.058	7098863.523	30.6
S24	769699.562	7092889.682	31.5
S65	777098.248	7096241.913	33.5

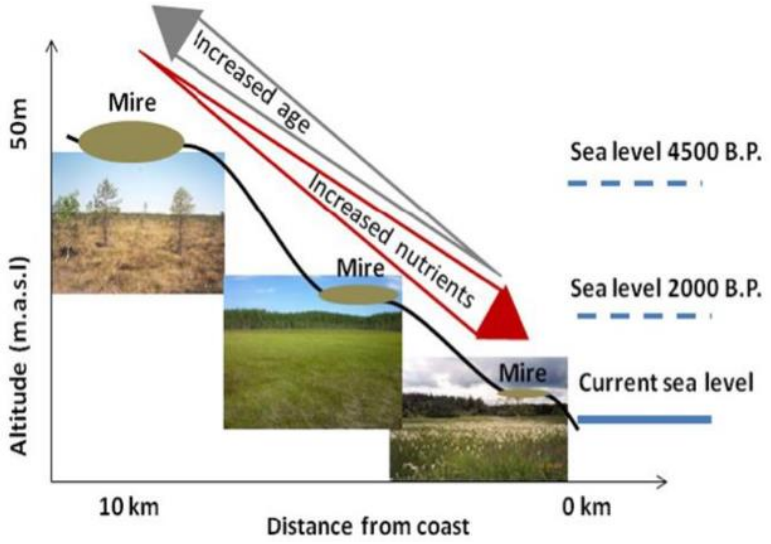

Figure 4. Schematic graph showing relationships between peatland (mire) age, elevation and geochemistry status in the study area

Sample Collection, Storage and Transport

Peat core samples were taken in early (20160620-20160704) and late (20160803-20160812) summer, from here on referred to as June and August sampling, respectively. Replicate samples were taken at 5 subplots within each peatland for a total of 75 sample subplot sites. A subplot consisted of a demarcated rectangle with area, 210 cm x 70 cm, whereby one third (70x70cm) was designated the control area, one third (70 cm x 70 cm) was designated the treatment area and a buffer area of equal size (70 cm x 70 cm) was included to separate control and treatment areas (Figure 5A). The result was 30 control samples (15 in June and 15 in August) and 15 treatment samples. In this report, only the 30 control samples will be considered.

In June, control samples were taken from 6 cm to 16 cm (i.e. 10 cm core samples) below the groundwater level in June at each subplot, to coincide with the assumed mean annual groundwater level (Figure 5, bottom left).

In August, control sampling was carried out in areas adjacent to but outside the control sample subplots demarcated in early summer to avoid potential confounding effects of the presence of the hole left by June sampling. To maintain the same sampling depth relative to groundwater level used in June, the difference between the groundwater depth in August and June was calculated. This difference was then added to the groundwater depth of this adjacent-to-control sample site to determine the depth for August sampling. The August control samples were taken from this depth to 10 cm below this depth (i.e. 10 cm core sample) (Figure 5, bottom middle and bottom right).

All 10 cm peat cores were divided in two (0-5 cm, referred to as L1, and 5-10 cm, referred to as L2). Each divided sample was placed in individual double airtight (Ziplock) bags before storage in the dark in a cold box (4°C), in which samples were transported to the laboratory for further preparation and analysis. From here on, the sampling period will be abbreviated with either J (June) or A (August) and the sampling depth with either L1 or L2. For example, JL1 will refer to peat core sampled at the shallow depth in June.

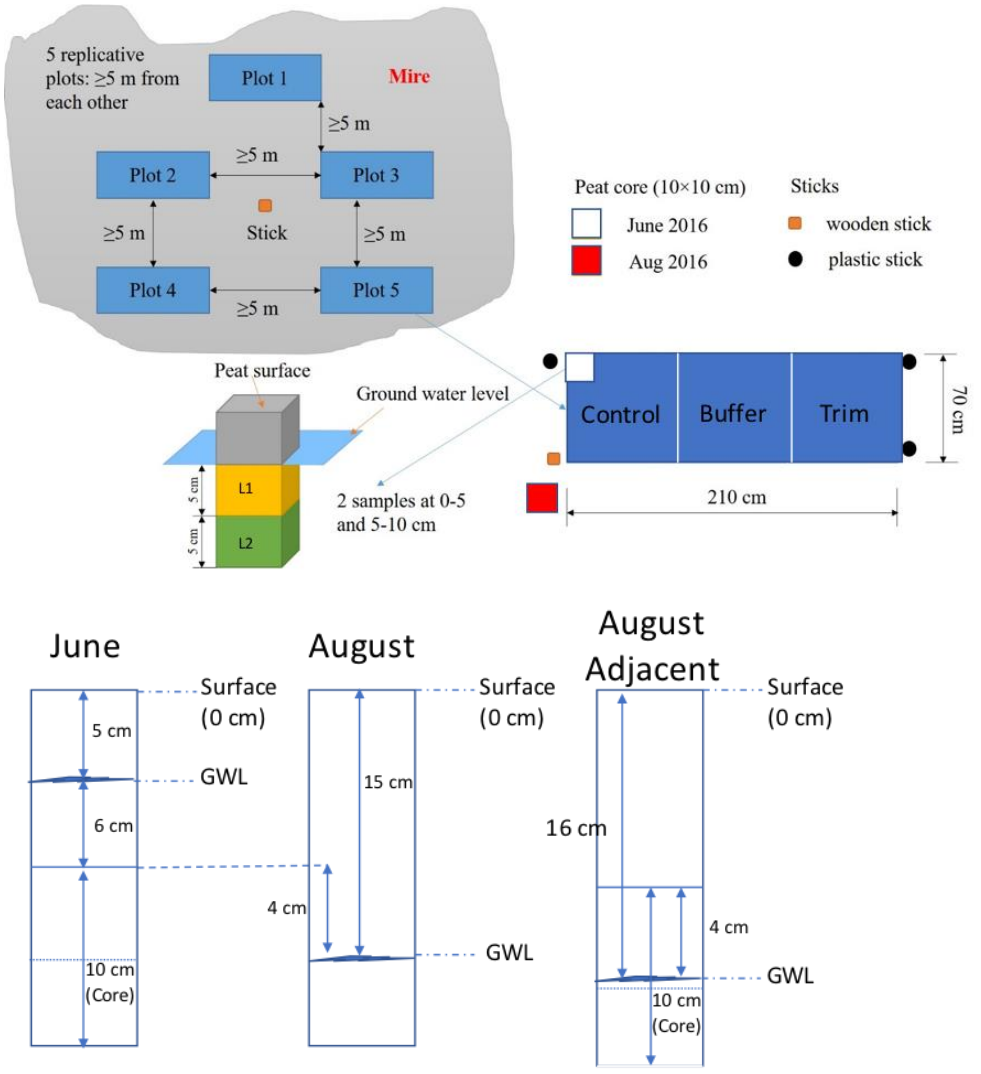

Figure 5. Schematic representations of the sampling protocol. Top: Subplots and subplot divisions in time and depth. Bottom: Determination of sampling depths, relative to groundwater level, at which core samples were taken. Values presented are example values from site S10.

Sample preparation and Hg, Major Soil Ions, and C and N analysis

Peat core samples of the five plots within each peatland with corresponding depth, treatment and sample period were homogenized prior to analysis. Pore water was squeezed out of each sample for pH measurement and homogenized samples were divided for the different analyses.

THg concentrations were determined by isotope dilution analysis by inductively coupled plasma mass spectrometry (ICPMS) with 196HgII as an internal standard. Samples were filtered at 45 µm followed by oxidation to Hg(II). Samples were then sequentially reduced, first to destroy any free halogens, then fully to convert Hg(II) to volatile Hg(0). Hg(0) was purged from solution and collected onto a gold trap then released and carried, via an inert gas, onto a second gold trap. After desorption from the second trap, a gas stream carried the Hg into the mass spectrometer. MeHg concentrations were determined by direct ethylation followed by a purge-trap step and detected after thermal desportion to isotope dilution analysis by Gas Chromatography-ICPMS (GC-ICPMS) analysis with Me196Hg as an internal standard. For both THg and MeHg signal deconvolution (Qvarnström and French, 2002) was used to calculate mass-bias corrected signals from the mass spectrometry results (Liem-Nguyen et al., 2016).

Solid peat amples were analysed for concentrations of major soil ions (Al, B, Ca, Fe, K, Mg, Mn, Na, P, S, Si, and Zn) by optical emission spectrophotometry with inductively coupled plasma (ICP-OES) using a Spectro Ciros Vision with gas pressure of > 7.5 bar argon (instrument quality) and plasma temperature 6000 - 8000 K (Supp. Table 1, see Appendix).

Samples were dried at 70°C for 18 hours before being analyzed for the mass fractions of C (ω_C) and N (ω_N). An Elemental analyzer (Flash EA 2000, Thermo Fisher Scientific, Bremen, Germany) was used in which C and N of the dried sample material was converted to CO_2 and N_2 by combustion and mass spectrometric measurement on CO_2 and N_2 yielded mass fractions. The results were corrected for drift and sample size effect (non-linearity). Working standards were wheat and maize flours calibrated against reference standards. For ω_N, atropine, cellulose, and NIST 1515 apple leaves. For ω_C, cyclohexanone, nicotinamide, and sucrose.

2.2 Geographic Information Systems Analysis

Geographic Data

A raster grid of 2m resolution elevation data (GSD-Höjddata, grid 2+ © Lantmäteriet?) of the study area was used as the basis for GIS analysis.
Översiktskartan, vector; Terrängkartan, vector; and Fastighetskartan med gränser, vector (all © Lantmäteriet) were used to identify land cover within the boundaries of the delineated watersheds. Similarly, Jordart 1: 25 000 - 1:100 000 (vector, © SGU) was used to identify soil type within the watershed boundaries.

Hardware

A MacBook Pro (Retina, 15-inch, Mid 2015) with a 2.2 GHz Intel Core i7 processor and 16 GB 1600 MHz DDR3 memory running OS X El Capitan was used for the majority the GIS analysis, except when ArcGis 10.4 was needed for which a Hewlet-Packard HP EliteDesk 800 G1 TWR (2013) was used with 8 GB RAM and intel(R) Core(TM) i7-4770 CPU @3.40GHz, 4 Cores running Microsoft Windows 10 Education.

Software

The open-source GIS Whitebox GAT (Lindsay, 2016) was used for watershed delineation and the subsequent calculation of area, slope, downslope index and curvature.

Arcgis 10.4 (ESRI?) was used in preparation of watershed delineation and area calculation, in particular, to transform coordinate systems when necessary as Whitebox does not include the SWEREFTM projection by default.

GIS workflow

Watershed delineation (Figure 6):

To define the upslope area contributing flow through each sampling site (i.e. watershed), the Watershed tool was used with inputs of a shapefile of points created from the GPS coordinates of the 15 sample sites to be used as pour points (watershed outlet points) and a breached 2m DEM of the study area (GSD-Höjddata, grid 2+ © Lantmäteriet). The breach depressions (Fast) tool was used to pre-process the DEM to remove areas of impeded or stagnating flow. The Jenson Snap Pour Points tool was used to align sample site points with the flow paths created with the D8 Flow Accumulation tool. In some instances, further manual adjustment was necessary and was done using the On-Screen Digitizing tool. All watersheds were carefully checked for impeding roads or ditches that would artificially limit their size but no such instances were observed.

The Area tool was used to calculate area, in m^2, of each of the 15 resulting watersheds (Supp. Fig. 1). For simplicity, watersheds will be referred to according to the sample site to which they provide input. For example, the watershed feeding to sample site S02 will be referred to as watershed S02.

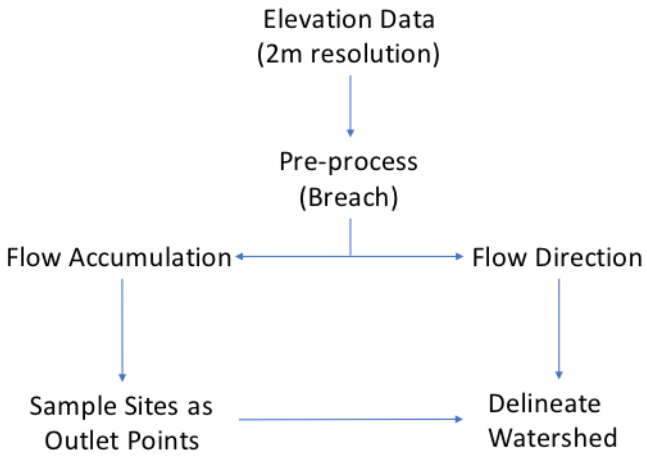

Figure 6. Workflow schematic of watershed delineation.

Soil type and land cover identification:
Relevant vector grids, mentioned above, were used to define the soil type and land cover type in the 15 watersheds. For instances where more than one type of soil and/or vegetation were present in a given watershed, the Clip and Area tools, in Whitebox, were used to calculate the areas of the different components of that watershed. Soil type and land cover data are presented as the ratio of component area:total watershed area.

Other geographic parameters:
The means of each watershed's Slope (Slope tool), Downslope Index (DSI) (Downslope Index tool, 1m vertical drop, tangent output), and Curvature (Total Curvature tool) were calculated to investigate their respective statistical relationships with Hg concentrations in the study. The original 2m resolution DEM was also resampled with the Aggregate tool to 10m, 20m, and 50m resolutions with the expectation that correlation between these three parameters and Hg concentrations may improve at resolutions closer to that of the peatlands themselves.

2.3 Statistical Analysis

The data from THg and MeHg, major ion, and C and N analyses were assembled and a subset of data for each of the sample depths and time periods was produced (i.e. one data subset for each of JL1, JL2, AL1, AL2). Statistical analysis was performed using the statistical software Minitab 17 or JMP 13 (SAS). Univariate linear regression was performed on each of the data subsets using Minitab. The four data subsets were reassembled for Principle Component Analysis (PCA) (Row-Wise Estimation Method) and Partial Least Squares (PLS) analysis (NIPALS Specification Method and Leave-One-Out Validation Method), using JMP 13. A significance level of $p < 0.05$ was used throughout.

3 Results

Watershed Delineation

Watersheds were defined by the upslope area contributing flow through the 15 sample sites, which were used as outlets for watershed delineation (Supp. Fig. 1). Potentially impeding structures, such as roads or ditches were looked for, but none were found that limited the extent of any of the delineated watersheds. Most of the delineated watersheds were small (n = 9 <500 m^2, n=13 <10,000 m^2 (1 ha)) (Table 2).

Table 2. *GIS parameters of 15 delineated watersheds*

Site ID	Elevation (m)	Area (m^2)	% Peatland	% Forest	Slope	DSI	Curvature
S02	0.9	79,104.00	31%	69%	2.26	0.0121	11.6
S70	1.5	1,116.00	62%	38%	2.90	0.0218	10.6
S43	3.3	9,624.00	17%	83%	2.47	0.0305	10.8
S13	3.5	16	100%	0%	0.43	0.0011	1.2
S10	4.8	12	100%	0%	0.28	0.0011	0.5
S52	10.1	22,376.00	34%	66%	2.51	0.0272	9.3
S14	14.1	356	100%	0%	0.25	0.0012	0.7
S18	14.6	16	100%	0%	0.76	0.0033	2.0
S16	14.6	4	100%	0%	0.59	0.0036	5.1
S62	15.6	36	100%	0%	0.39	0.0022	1.0
S29	27.2	1,132.00	100%	62%	1.10	0.0032	8.6
S26	28.9	5,336.00	100%	10%	1.31	0.0027	8.2
S33	30.6	464	100%	0%	0.58	0.0024	3.6
S24	31.5	328	100%	0%	0.66	0.0057	4.4
S65	33.5	104	100%	0%	0.52	0.0027	1.1

Watershed area generally decreased with increasing elevation, which can largely be explained by proximity of higher elevation sites to watershed divides and therefore limited watershed area. A consequence of the overrepresentation of small watersheds was a constraint on the fraction of non-peatland land cover in the watersheds, with the 9 highest-elevation watersheds consisting of 100% peatland. Similarly, non-peatland land cover (i.e. Forest), was only present in the largest watersheds, while large Slope, Downslope Index and Curvature values were also associated with large watershed area.

GIS Parameters vs. Hg concentrations

Despite the limitations in the results of the GIS analysis, linear regression analysis was carried out to compare the GIS parameters and the Hg data (Table 3, 4, 5; Figure 7, 8, 9). THg concentration (Table 3, Figure 7) and the MeHg:THg ratio (Table 5, Figure 9) correlated significantly with Elevation, in particular in August (AL1, AL2), but no significant correlation was found between MeHg concentration and Elevation (Table 4, Figure 8). No significant correlations were found between Hg and any of the other GIS parameters (Area, % Peatland, % Forest, Slope, Downslope Index, or Curvature). The expectation that calculating Slope, Downslope Index, and Curvature on a scale that would more accurately represent that of the study peatlands would provide more meaningful results led to the resampling of the original DEM to decrease grid cell resolution to 10 m, 20 m, and 50 m. These three GIS parameters were recalculated at these new resolutions, but still no significant correlations between these parameters and Hg concentrations were observed (Data not shown).

Table 3. *Linear regression analysis of THg concentrations and GIS Parameters*

THg	**JL1**		**JL2**		**AL1**		**AL2**	
	r	**P**	**r**	**P**	**r**	**P**	**r**	**P**
Elevation	***0.545***	***0.036***	0.372	0.172	***0.767***	***0.001***	***0.645***	***0.009***
Area (m^2)	-0.005	0.985	0.043	0.879	-0.197	0.482	-0.223	0.423
% Peatland	0.215	0.441	0	1	0.39	0.151	0.316	0.251
% Forest	-0.169	0.547	-0.089	0.753	-0.314	0.254	-0.326	0.235
Slope	0.204	0.467	0.143	0.612	-0.011	0.97	0.139	0.621
DSI	0.15	0.593	0.225	0.419	0.047	0.869	0.199	0.478
Curvature	0.204	0.467	0.179	0.524	-0.025	0.93	0.054	0.85

Significant correlation denoted by bold and italic text in all relevant tables.

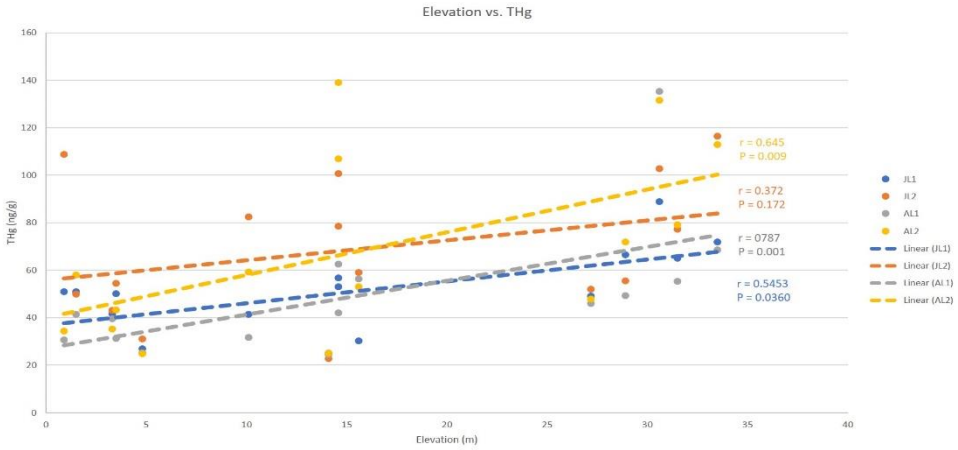

Figure 7. Correlations of elevation vs. THg for the different sampling dates and depths

Table 4. *Linear regression analysis of MeHg concentrations and GIS Parameters*

MeHg	**JL1**		**JL2**		**AL1**		**AL2**	
	r	**P**	**r**	**P**	**r**	**P**	**r**	**P**
Elevation	-0.327	0.234	-0.173	0.537	-0.374	0.17	-0.206	0.462
Area (m^2)	-0.045	0.874	-0.354	0.196	0.155	0.58	-0.141	0.616
% Peatland	-0.179	0.524	0	1	-0.353	0.197	-0.138	0.625
% Forest	-0.113	0.689	-0.318	0.248	0.089	0.753	-0.141	0.616
Slope	-0.082	0.771	-0.2	0.475	0.082	0.771	-0.075	0.791
DSI	0.009	0.975	-0.066	0.815	0.163	0.562	0.136	0.629
Curvature	-0.011	0.97	-0.25	0.369	0.186	0.508	0.029	0.919

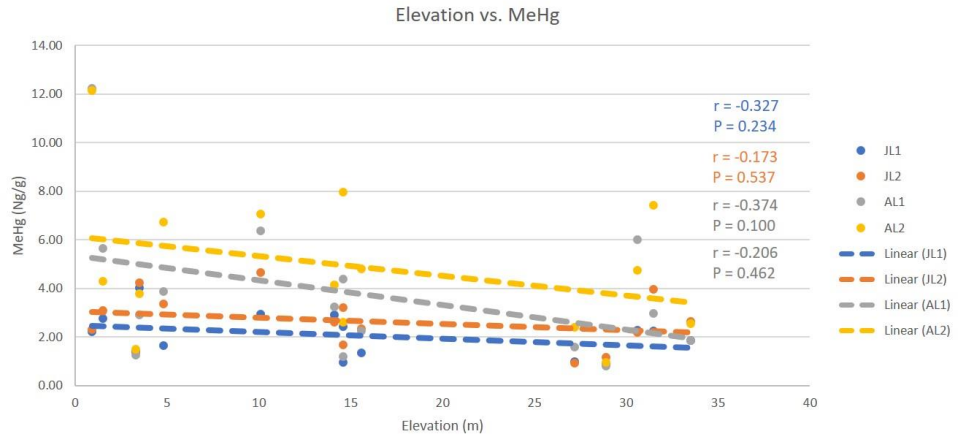

Figure 7. Correlations of elevation vs. THg for the different sampling dates and depths

Table 5. *Linear regression analysis of MeHg:THg ratios and GIS Parameters*

MeHg:THg	**JL1**		**JL2**		**AL1**		**AL2**	
	r	**P**	**r**	**P**	**r**	**P**	**r**	**P**
Elevation	-0.361	0.229	-0.349	0.203	***-0.647***	***0.009***	***-0.522***	***0.046***
Area (m^2)	-0.132	0.638	-0.331	0.229	0.105	0.708	0.043	0.879
% Peatland	-0.197	0.481	0.014	0.961	-0.394	0.146	-0.261	0.347
% Forest	-0.093	0.743	-0.25	0.369	0.157	0.576	0.064	0.819
Slope	-0.293	0.289	-0.364	0.182	0.036	0.899	-0.182	0.516
DSI	-0.197	0.482	-0.243	0.382	0.082	0.771	-0.05	0.859
Curvature	-0.246	0.376	-0.418	0.121	0.118	0.676	-0.075	0.791

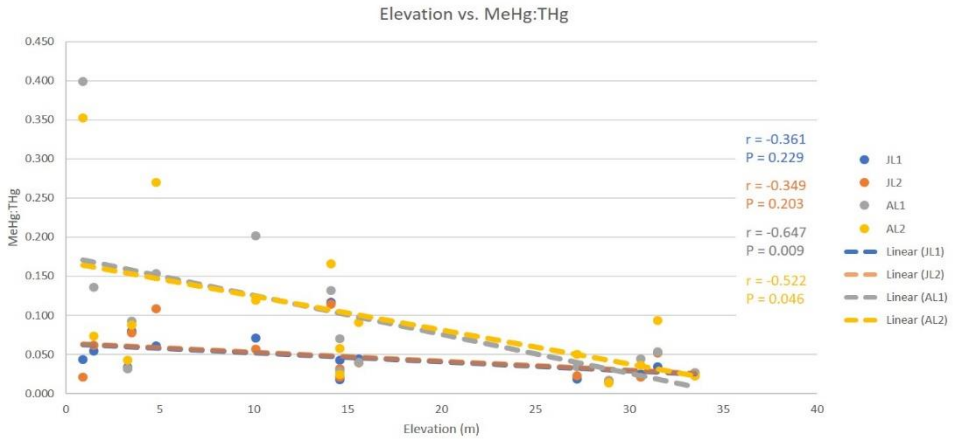

Figure 9. Correlations of elevation vs. MeHg:THg for the different sampling dates and depths

Peat Core Major Ion Concentrations vs. Hg concentrations

While significant correlation was absent between most GIS parameters and Hg concentrations, the roles of chemical compounds in the peat samples were investigated and the relationships found can be said to conform to the findings of previous studies (Hintelmann, Welbourn and Evans, 1995; Grigal, 2003; Fleming et al., 2006, Ding et al., 2009, Demers et al., 2013). The soil ion chemistry of the two depths of sampling at both time-points were each analysed independently for statistically significant relationships with Hg concentrations (Table 6, 7, 8). Description of these relationships will be brief, however, as they are outside the main scope of this report.

Along with elevation, at JL1, THg concentrations showed significant correlation with K, N, and C, whereas for JL2, significant correlations were found with Al, S, N, and C:N (Table 6). The correlations with N, C, and S likely represent association with soil organic matter as expected. In August, the relationship between THg and S became non-significant but strong correlations with N and C continued.

In contrast to THg, MeHg at JL1 more closely related to biologically relevant factors such as high pH and S concentrations (and Fe concentrations although just below significance), and low C:N (Table 7). High pH and low C:N tend to promote microbial activity, while the correlations with S and Fe suggest the active presence of SRBs and IRBs, which would act in Hg methylation.

At AL1, MeHg continued to correlate with compounds more associated with biological activity than THg. MeHg correlated significantly with pH, Ca, P, Si, Zn and, importantly, S. Correlation between MeHg and Fe also increased to become strongly significant, which was not the case in in June. With increasing temperatures over the summer months, microbial activity tends to increase, which would include Hg methylation. The associations discovered here in August are likely a consequence of that.

In June, MeHg:THg correlated positively with pH, Ca, K, Mg, and Mn, as well as negatively with Elevation, indicating Hg methylators were particularly active in the ion-rich soils nearer to the coast/at low elevation (Table 8). These associations continued to hold later in August along with the inclusion of a strong correlation with Na, again implying a relationship between a large MeHg:THg ratio and proximity to the coast where ion-rich, low elevation soils were present.

Table 6. *Linear correlates of THg concentrations*

THg	**JL1**		**JL2**		**AL1**		**AL2**	
	r	**P**	**r**	**P**	**r**	**P**	**r**	**P**
pH	-0.361	0.186	-0.023	0.934	***-0.632***	***0.012***	-0.432	0.108
MeHg	-0.146	0.603	0.064	0.82	-0.2	0.475	0.032	0.909
MeHg:THg	-0.443	0.098	-0.611	0.016	-0.611	0.016	-0.636	0.011
Al	0.014	0.96	***0.568***	***0.027***	0.386	0.156	0.229	0.413
B	0.062	0.827	0.371	0.173	*	*	*	*
Ca	-0.371	0.173	-0.179	0.524	-0.5	0.058	-0.425	0.114
Fe	-0.018	0.95	0.304	0.271	-0.089	0.752	-0.164	0.558
K	***-0.686***	***0.005***	-0.393	0.147	***-0.689***	***0.004***	***-0.804***	***0***
Mg	-0.425	0.114	-0.332	0.226	***-0.793***	***0***	***-0.664***	***0.007***
Mn	***-0.496***	***0.06***	-0.162	0.565	***-0.6***	***0.018***	***-0.668***	***0.007***
Na	-0.264	0.341	-0.057	0.84	-0.439	0.101	-0.221	0.428
P	0.182	0.516	0.5	0.058	-0.225	0.42	0.257	0.355
S	0.304	0.271	***0.536***	***0.04***	0.104	0.713	0.443	0.098
Si	-0.407	0.132	-0.073	0.795	-0.332	0.226	-0.068	0.81
Zn	0.218	0.435	0.206	0.461	0.418	0.121	0.036	0.899
N	***0.544***	***0.036***	***0.811***	***0***	0.22	0.431	***0.699***	***0.004***
C	***0.518***	***0.048***	0.182	0.516	***0.746***	***0.001***	***0.679***	***0.005***
C/N	-0.496	0.06	***-0.664***	***0.007***	-0.196	0.483	-0.454	0.089
GW(Jun)	0.508	0.053	0.286	0.301	-0.104	0.713	0.25	0.368
GW(Aug)	*	*	*	*	0.369	0.177	0.369	0.177

*In tables 6, 7, and 8, * represents absence of dating (B below detection limit, (Supp. Table 1).)

Table 7. *Linear correlates of MeHg concentrations*

MeHg	**JL1**		**JL2**		**AL1**		**AL2**	
	r	**P**	**r**	**P**	**r**	**P**	**r**	**P**
pH	***0.646***	***0.009***	0.496	0.06	***0.774***	***0.001***	***0.608***	***0.016***
THg	-0.146	0.603	0.064	0.82	-0.2	0.475	0.032	0.909
MeHg:THg	-0.089	0.752	***0.689***	***0.004***	***0.868***	***0***	***0.718***	***0.003***
Al	0.129	0.648	0.186	0.508	0.375	0.168	0.557	0.031
B	0	1	-0.124	0.66	*	*	*	*
Ca	***0.746***	***0.001***	***0.579***	***0.024***	***0.729***	***0.002***	***0.614***	***0.015***
Fe	0.493	0.062	0.396	0.143	***0.779***	***0.001***	***0.543***	***0.037***
K	0.221	0.428	0.35	0.201	0.264	0.341	0.254	0.362
Mg	***0.525***	***0.044***	0.454	0.089	***0.579***	***0.024***	0.364	0.182
Mn	***0.568***	***0.027***	0.41	0.129	***0.582***	***0.023***	0.443	0.098
Na	-0.039	0.889	0.375	0.168	0.475	0.074	***0.725***	***0.002***
P	0.5	0.058	0.261	0.348	***0.65***	***0.009***	0.486	0.066
S	***0.679***	***0.005***	***0.543***	***0.037***	***0.746***	***0.001***	***0.532***	***0.041***
Si	***0.707***	***0.003***	0.309	0.262	***0.746***	***0.001***	0.511	0.052
Zn	-0.306	0.268	-0.226	0.418	***-0.657***	***0.008***	-0.5	0.058
N	0.369	0.177	0.054	0.85	0.512	0.051	0.306	0.268
C	-0.343	0.211	-0.343	0.211	-0.489	0.064	-0.336	0.221
C/N	***-0.604***	***0.017***	-0.357	0.191	***-0.568***	***0.027***	-0.289	0.296
GW(Jun)	0.016	0.955	0.208	0.458	-0.243	0.382	-0.004	0.99
GW(Aug)	*	*	*	*	-0.107	0.703	0.106	0.708

Table 8. *Linear correlates of MeHg:THg concentrations*

MeHg: THg	**JL1**		**JL2**		**AL1**		**AL2**	
	r	**P**	**r**	**P**	**r**	**P**	**r**	**P**
pH	***0.708***	***0.003***	0.348	0.203	***0.886***	***0***	***0.762***	***0.001***
THg	-0.443	0.098	***-0.611***	***0.016***	***-0.611***	***0.016***	***-0.636***	***0.011***
MeHg	-0.089	0.752	***0.689***	***0.004***	***0.868***	***0***	***0.718***	***0.003***
Al	-0.432	0.108	-0.161	0.567	0.118	0.676	0.211	0.451
B	-0.371	0.173	-0.371	0.173	*	*	*	*
Ca	***0.736***	***0.002***	***0.564***	***0.028***	***0.804***	***0***	***0.8***	***0***
Fe	-0.250	0.369	0.196	0.483	***0.618***	***0.014***	***0.525***	***0.044***
K	***0.714***	***0.003***	***0.604***	***0.017***	***0.557***	***0.031***	***0.739***	***0.002***
Mg	***0.686***	***0.005***	0.496	0.06	***0.793***	***0***	***0.714***	***0.003***
Mn	***0.707***	***0.003***	0.496	0.06	***0.764***	***0.001***	***0.804***	***0***
Na	-0.350	0.201	0.404	0.136	***0.639***	***0.01***	***0.736***	***0.002***
P	-0.393	0.147	-0.068	0.81	***0.525***	***0.044***	0.211	0.451
S	-0.500	0.058	-0.032	0.909	0.457	0.087	0.096	0.732
Si	***0.700***	***0.004***	0.365	0.181	***0.643***	***0.01***	0.496	0.06
Zn	-0.49	0.064	-0.409	0.13	***-0.743***	***0.002***	-0.471	0.076
N	-0.508	0.053	***-0.575***	***0.025***	0.215	0.442	-0.225	0.42
C	***-0.536***	***0.04***	-0.418	0.121	***-0.743***	***0.002***	***-0.732***	***0.002***
C/N	***0.514***	***0.05***	0.15	0.594	-0.268	0.334	0.046	0.869
GW(Jun)	-0.027	0.924	-0.186	0.507	-0.186	0.507	-0.186	0.507
GW(Aug)	*	*	*	*	-0.195	0.486	-0.188	0.503

Relative change in Hg

The change in THg and MeHg concentrations and MeHg:THg ratio were calculated as the change in values from August relative to those in June. THg concentrations decreased between sampling dates for the 6 lowest elevation sample sites (Figure 10, top). The opposite trend was not as clear as both increases and decreases were seen in higher elevation sites. For most sites, changes in the same direction occurred at both depths, but again more variation was present at higher elevations.

Nearly all sites experienced increases in MeHg concentrations, with 8 sites having increases of >100% at least one depth (Figure 10, middle). Increases at S02 were especially strong. Sites S43, S13, S26, and S65 did not show large increases over the summer. Instead, these sites showed no change or small decreases in MeHg concentration. These four sites are separated evenly between the low- and high-elevation classes and are distributed seemingly randomly across the study area (Supp. Fig. 2), making it difficult to deduce explanations for these results.

Trends in changes in the MeHg:THg ratio were similar to those described for changes in MeHg concentration. The most striking finding was the exceptional increase at site S02 at both depths but at the greater depth in particular (Figure 10, bottom). Despite the fairly consistent trends of decreases in THg concentrations at low-elevation sites and increases in MeHg concentrations at nearly all sites, no other site approached the massive increases in MeHg:THg seen at S02. Several sites show increases > 100% but none exceeded 200%.

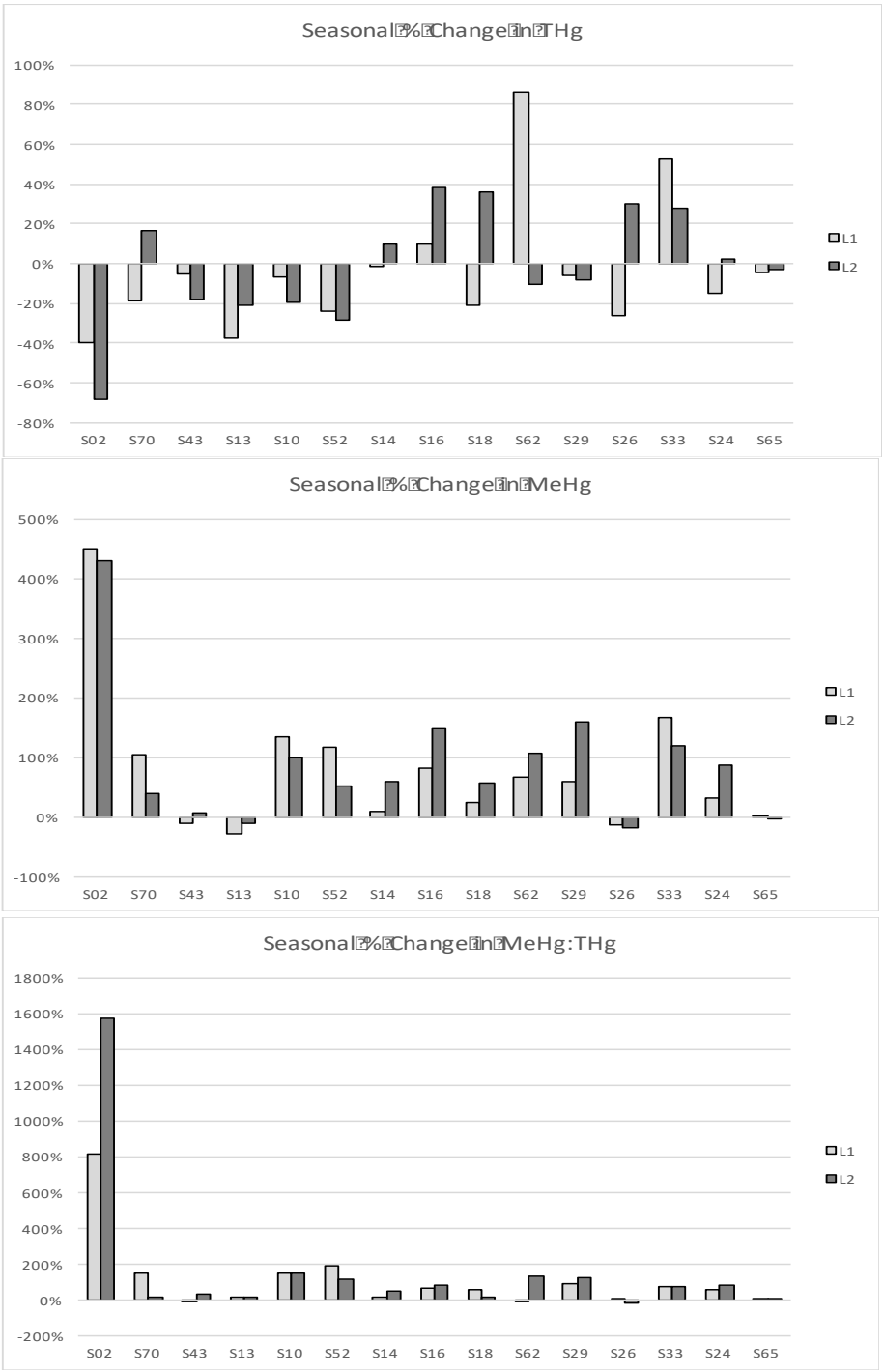

Figure 10. Relative change top left: THg concentrations, top right: MeHg concentrations, bottom: MeHg:THg ratio at both sampling depth of the 15 sample sites. Note differences in Y-axes.

Multivariate analysis

PLS:

Partial Least Squares analysis of data from all sample depths and time periods pointed to pH, Ca, Fe, Mg, Na, P, S, Si, and Watershed Area as the parameters with the highest Variable Importance Projections (VIPs) in the fitted model for MeHg (VIP>1, Figure 11).

For THg, the important variables were Elevation, Al, Mg, Mn, S, N, C, C:N and Groundwater level in June. Despite the large regression coefficient of pH in the THg model, its VIP was just below the cutoff (VIP = 0.982).

For the model fitted to the MeHg:THg ratio, the important variables were pH, Fe, K, Mg, Na, C, and Watershed Area.

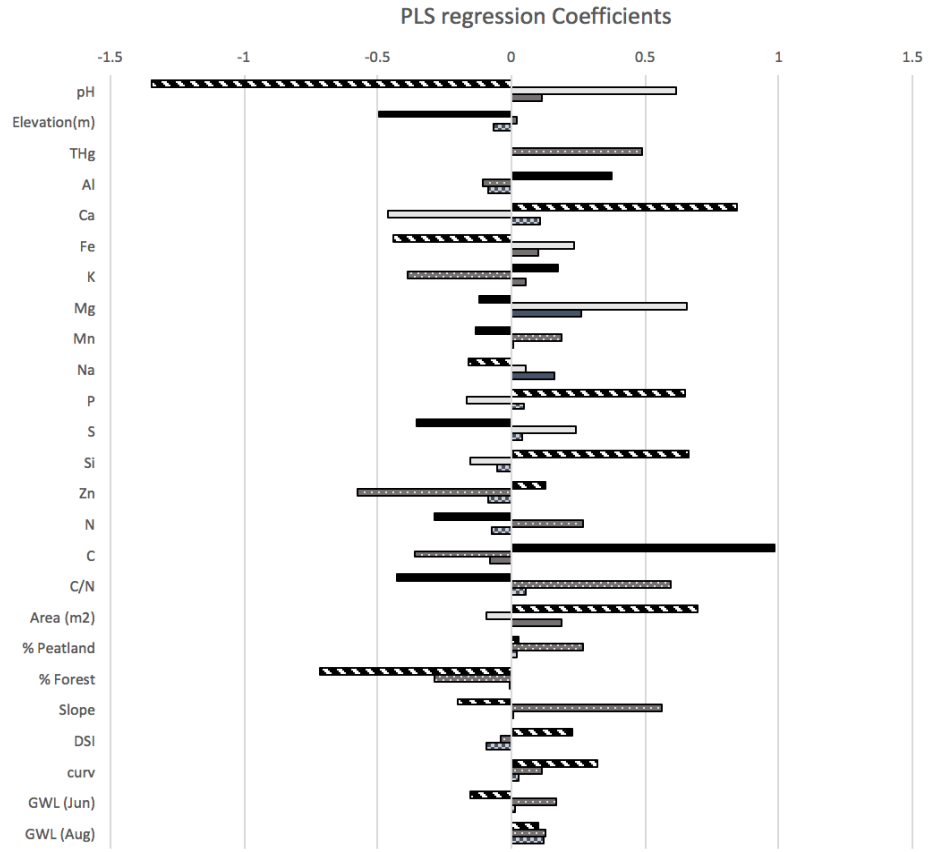

Figure 11. Partial Least Squares regression coefficients of all parameters as they contribute to variation in THg (black and white angled stripes), MeHg (light gray dots), MeHg:THg (middle gray checkers). Solid bars: VIP, Patterned bars: VIP<1

While results from the PLS analysis were generally similar to those of the univariate linear regression, the importance of Watershed Area for MeHg and the

MeHg:THg ratio was a new development. Although in support of associations between geographic characteristics of a watershed and Hg concentrations at its outlet, this link points away from the simplistic initial hypothesis of Elevation as the major explanatory variable.

PCA:

Principle component analysis revealed that the majority of sample sites were similar as they grouped together in the centre of the plots comparing PC1 and PC2, and PC1 and PC3 (Figure 12, Top and Bottom, respectively). The exceptions were S02, S52, and to a lesser extent, S43, and S70.

Concentrations of MeHg, pH, Al, Fe, Mg, Na, P, S, Si and N at S02 were regularly the highest or among the highest compared to other sites while C and C:N were often among the lowest (Supp. Table 1). MeHg concentration was extremely high in August, with THg very high at JL2. S52 also showed consistently extreme values for several parameters across depth and time. Of note were high values for pH, Ca, Fe, K, Mg, Mn, P, S, Si, and N, and low values for C and C:N (Supp. Table 1). S02 and S52 had the two highest concentrations of S. Values at S43 and S70 were also regularly high (Supp. Table 1).

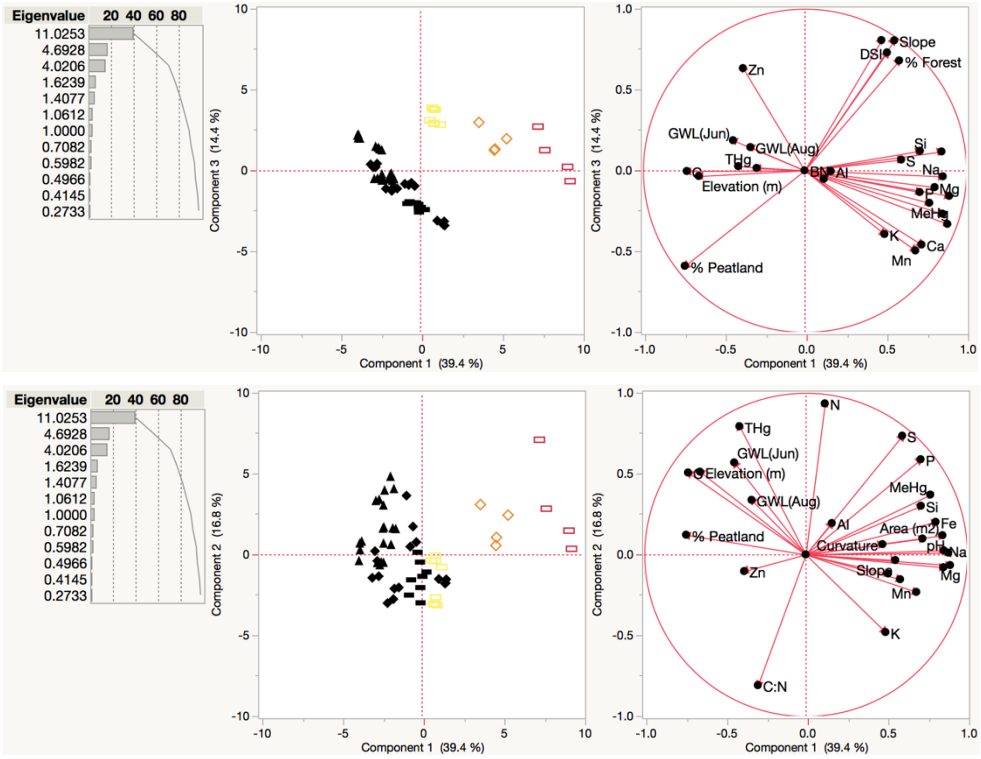

Figure 12. Principle component analysis of data from all time points and depths. Top: PC1 and PC2, Bottom: PC and PC3. Circles: Low-elevation group, Squares: Mid-elevation group, Triangles: High-elevation group. Red Hollow: S02, Orange Hollow: S52, Yellow hollow: S43 and S70

While extreme values for several parameters were common among the sampling sites, S02, S52, S43 and S70, their associated Watershed Areas were also among the largest (ranked 1st, 2nd, 3rd, and 6th, respectively). Thus, in both of the multivariate analyses, watershed area is suggested as a key parameter that associates with Hg concentrations, in particular, regarding extreme values, as in the PCA.

Although limitations in the distribution of the watershed area data limited the potential for a more refined model for prediction of Hg in peatlands in the study area, these results clearly point to a link between large watershed area and major ion concentrations, including MeHg. Not only do these "extreme" value sample sites receive input from larger watersheds, the larger watershed itself allows for a larger proportion of forest in the watershed, with forest vegetation and soil more prone to accumulation and therefore acting as an eventual source to peatlands.

Watersheds S26 and S29, for example, are both larger than S43 but they are comprised entirely of peatland (Table 2). Forest is known to provide Hg to peatlands where methylation more readily occurs, but the results of this study imply that the % Forest in a watershed may be a good predictor of extreme concentrations. The relationship, however, is complex: S43 has the 3rd largest area and higher % Forest than S02 or S52 but has generally the lowest major ion concentrations among the "extreme" sites. S70 has the smallest watershed of the "extreme" sites and the lowest % Forest but has generally higher ion concentrations than S43 though still lower than S02 or S52.

While S02 and S52 likely have the highest major ion concentrations simply because they have by far the largest watershed, that their % Forest values lie between those of the other "extreme" sites may indicate a goldilocks range for % Forest. For such extreme values to be present, a balance may need to be struck between the fraction of a watershed that is forested, which provides major ions to a peatland, and the fraction that is peatland and receives that input. Too large a peatland:forest ratio will lead to low "catchment" inputs to the peatland, whereas too high a ratio will lead to overloading of the peatland. In the latter case, the ions may bypass the peatland in preferential flow paths without having a chance to accumulate. The veracity and relevance of these dynamics cannot be assured, however, based on the limited number of sites in which they are present in this study.

A second trend that can be observed when comparing PC1 and PC3, was the shift of the four "extreme" sites towards the grouping of vectors describing % Forest, Slope, DSI, and Curvature, and away from % Peatland. The relative proximity of these extreme sites and these GIS parameters acts to reinforce the conclusion that watersheds of sufficiently large size, and which therefore contain non-peatland land cover types, are likely to have higher values of major ions, including MeHg.

H*ypothetical Sample Sites*

Because of the limitations of the GIS parameter data caused by the strong skewedness of the distribution of watershed areas, an exercise in GIS was carried out to try to identify a new series of 15 sample sites that might have provided enough variation to enable more meaningful conclusions than the sites used in this study.

These new hypothetical sites were selected from the nearly 70 sample sites from which this study's actual sites were chosen and a watershed was delineated for each of them. 15 sites were identified that would correspond to the 15 largest watersheds (5 from each of the 3 previously defined elevation classes), excluding watersheds nested within other watersheds (Table 9). Four of the sites used in this study were present in the new list of sites, with one in each of the low- and mid-elevation class and two in the high-elevation class. Two watersheds greater than approximately 20000 m^2 exist in each of the three elevation classes, whereas, in the original sites, only two such watersheds were present (S02 and S52) among all 15 sites. In the original sites, watersheds > 1000 m^2 were large enough to contain land cover other than 100% peatlands. Among the new sites, only two sites less than 1000 m^2 exist, one in each of the mid- and high-elevation classes and none in the low class. If watersheds with area within the range of 1000 m^2 and 20000 m^2 (arbitrary thresholds) can be considered mid-size, two such watersheds exist in each of the mid- and high-elevation classes and three in the low class. A more robust distribution of watershed area as well as land cover type was achieved with these new sites.

Table 9. Hypothetical sample sites

Current Site	Elevation	Area (m^2)	% Peatland	% Forest
S07	0.7	6208	67%	33%
S02*	0.9	79104	31%	69%
S04[c]	1.5	2644	37%	64%
S45	3.2	89416	16%	84%
S09	5.1	3400	24%	76%
S52*	10.1	22376	34%	66%
S15	13.9	628	100%	0%
S20	14.5	38328	71%	80%
S19	14.6	4324	100%	0%
S63[c]	15.6	3972	3%	97%
S30[i]	26.6	85232	46%	54%
S58	27.9	1968	98%	2%
S26*	28.9	5336	100%	10%
S33*	30.6	464	100%	0%
S56	36.0	25224	12%	88%

*Sites present in current study; [c]Large portions of forest cut down; [i]Watershed impeded by road

4 Discussion

The significant correlations between Elevation and both THg and MeHg:THg, revealed by linear regression, can be considered an initial insight into the relationship between Hg and mire age in the peatlands of these forested catchments in northern Sweden. Elevation along the chronosequence, created by land rise where elevation is proportional to time since emergence from the Baltic Sea, was the first inference of validity for the hypothesis that underlying peatland age influences Hg concentrations and mercury methylation across the study area, via effects on the accumulation or loss of substances from the peat and the development of the peat ecosystem with time.

Elevation alone, however, was far from able to adequately explain the patterns in Hg concentration, the major failing being the lack of correlation with MeHg concentrations. Furthermore, the importance of THg in defining methylation rates has been brought into question in previous studies (Bergman et al., 2012, Åkerblom et al., 2013).

For these reason, relationships with geographic parameters (Watershed area, % wetland, % forest, slope, downslope index, curvature) in the catchment areas of the study plots were investigated, starting with the delineation of watersheds for funneling to these sites. Watershed Area was the only parameter in the catchment identified as contributing to a PLS model explaining trends in MeHg concentrations and MeHg:THg ratio. None of the geographic parameters contributed to the model for THg. Watershed area can therefore be said to provide more insight into MeHg concentrations than elevation alone.

The overrepresentation of small watersheds (n = 9 <500m^2, n=13 <10,000m^2 (1 ha)) may have obscured a greater understanding of patterns in Hg concentrations with respect to watershed area and other GIS parameters. However, the results of this study do reveal that sites with watersheds large enough to contain land cover other than 100% peatland (i.e. include forest) tended to have higher THg and MeHg concentrations along with other major ions.

A further hindrance in this study's attempt to explain trends in Hg was the failure of a key assumption, namely the expected inverse relationship between Elevation and Sulfur concentration. Both THg and MeHg are known to coincide spatially with sulfur either by association sulfur in organic matter (Xia et al., 1999; Qian et al., 2002) or during sulfate reduction by sulfate-reducing bacteria (Bartha and Campeau 85; Demers et al., 2013). The presence of a Sulfate gradient may have been overlooked, however due to insufficiently specific Sulfur and soil type data. Hg methylation would be expected to correlate strongly with Sulfate concentrations in the peat but not necessarily with other forms that would be included in the Total Sulfur data used in this study. Meanwhile, sulfate reduction itself is known to

closely associate with fine-grain sediment from what was once the sea floor (Westrich, 1983). This type of sediment would be expected more in the low-elevation sites. A more detailed investigation into soil grain size and the relationship between fine-grain soil material, sulfur, and MeHg may reveal the presence of a gradient of Sulfur in the watersheds, which may bring forward stronger relationships with Hg concentrations.

Despite the absence of the expected S gradient with elevation, MeHg concentrations did correlate with S concentrations, especially at the shallow sampling depth (L1). This finding is in line with published literature as SRBs are considered the dominant mediators of Hg methylation (Campeau and Bartha 85, Xia et al., 1999).

The absence of coincident Elevation and Sulfur gradients along the chronosequence was a hindrance to the full acceptance of a hypothesis of this study but the greater threat to the analysis was indeed the distribution of the areas of the delineated watersheds with sample sites as their outlets. With 13 of the 15 watershed areas less than 1 ha and 9 less than 500m^2, little of meaning could be concluded from statistical analysis with certainty. Linear regression and PLS pointed to Elevation's relationship with THg, PLS implicated Watershed Area as being associated with MeHg, and PCA hinted at the relevance of Area as well as a cluster of Slope, Downslope Index, Curvature, and % Forest for sample sites with extreme values of Hg and other metals, but the multivariate analyses relied heavily on the chemical data as opposed to the geographic.

Utilizing the powers of hindsight, a hypothetical rethink of the design of the experiment that was the basis for this study was carried out with the aim to identify 15 sample sites that could have been used and may have avoided the drawbacks of the current set of study sites. The limitations of the actual sites were several but most lay in the overrepresentation of small watersheds, which consisted entirely of peatlands (without forest or other land cover types). These watersheds stunted analysis due to a lack of variation between them. Most of the watersheds possessed similar patterns of land cover, limiting their use as explanatory variables. Among watersheds with varying land cover, distribution across the 3 elevation classes was uneven and further limited their use in the statistical analysis.

The delineation of Watershed Area is itself prone to uncertainty based on inaccuracies in the DEM derived from satellite imagery as well as biases in the algorithms used during delineation and subsequent watershed-scale calculations (Woodrow, Lindsay and Berg, 2016). While the presence of uncertainty is important to consider when interpreting the results of this study, its nature was not covered, as a parallel study will be carried out on the subject.

It is my recommendation, therefore, that in similar, future projects, GIS analysis should be performed during the initial phase of, and provide basis for, experimental design rather than during post hoc analysis.

5 Conclusions

Univariate linear regression seemed to indicate no relationship between elevation or any of the other geographic characteristics of watersheds and MeHg. However, the strongly skewed distributions of the GIS parameters, a result of the extremely small size of most watersheds, called into question the power and relevance of univariate regression analysis in this context.

Multivariate analyses (Partial Least Squares and PCA) pointed to Watershed Area as an important variable in the fitted models aiming to explain both MeHg concentration and the MeHg:THg ratio. Unfortunately, the skewedness of the parameters again calls these findings into question as it cannot be known, without further study, if the relationships between them and Hg concentrations are an artefact of the skewedness or if the skewedness is, in contrast, masking stronger, potentially significant relationships.

Hints of the potential of geographic characteristics to predict, or at least help to explain, Hg concentrations and transformations appeared at certain instances throughout the analyses of this study but given the limitations of the experimental design, the significance of their roles cannot be fully gleaned in this study. Including watershed delineation in the experimental design stage of this study may have enabled more definitive conclusions. Our results indicate that elevation alone is not a strong predictor of MeHg concentration, however.

References

Amirbahman, A., Fernandez, I.J., 2012. The Role of Soils in Storage and Cycling of Mercury, in: Mercury in the Environment, Pattern and Process. University of California Press, pp. 99–118.

Bergman, I., Bishop, K., Tu, Q., Frech, W., Åkerblom, S., Nilsson, M., 2012. The Influence of Sulphate Deposition on the Seasonal Variation of Peat Pore Water Methyl Hg in a Boreal Mire. PLOS ONE 7, e45547. doi:10.1371/journal.pone.0045547

Bernhoft, R.A., 2012. Mercury Toxicity and Treatment: A Review of the Literature. Journal of Environmental and Public Health 2012, 460508. doi:10.1155/2012/460508

Bishop, K., Lee, Y.-H., Pettersson, C., Allard, B., 1995. Terrestrial sources of methylmercury in surface waters: The importance of the riparian zone on the Svartberget Catchment. Water, Air, and Soil Pollution 80, 435–444. doi:10.1007/BF01189693

Chrystall, L., Rumsby, A., 2008. Mercury Inventory for New Zealand 2008 (Prepared for the Ministry for the Environment of New Zealand). Pattle Delamore Partners Limited, pp. 10.

Compeau, G.C., Bartha, R., 1985. Sulfate-Reducing Bacteria: Principal Methylators of Mercury in Anoxic Estuarine Sediment. Applied and Environmental Microbiology 50, 498–502.

Demers, J.D., Driscoll, C.T., Fahey, T.J., Yavitt, J.B., 2007. Mercury cycling in litter and soil in different forest types in the adirondack region, New York, USA. Ecological Applications 17, 1341–1351. doi:10.1890/06-1697.1

Demers, J.D., Yavitt, J.B., Driscoll, C.T., Montesdeoca, M.R., 2013. Legacy mercury and stoichiometry with C, N, and S in soil, pore water, and stream water across the upland-wetland interface: The influence of hydrogeologic setting. J. Geophys. Res. Biogeosci. 118, 825–841. doi:10.1002/jgrg.20066

Ding, Z.H., Liu, J.L., Li, L.Q., Lin, H.N., Wu, H., Hu, Z.Z., 2009. Distribution and speciation of mercury in surficial sediments from main mangrove wetlands in China. Marine Pollution Bulletin 58, 1319–1325. doi:10.1016/j.marpolbul.2009.04.029

Driscoll, C.T., Yan, C., Schofield, C.L., Munson, R., Holsapple, J., 1994. The mercury cycle and fish in the Adirondack lakes. Environ. Sci. Technol. 28, 136A–143A. doi:10.1021/es00052a003

EEC. 1992. Council Directive 92/43/EEC of 21 May 1992 on the conservation of natural habitats and of wild fauna and flora. *OJ L 206, 22.7.1992, p. 7–50*

ESRI 2011. ArcGIS Desktop: Release 10. Redlands, CA: Environmental Systems Research Institute.

Fischer, R.G., Rapsomanikis, S., Andreae, M.O., Baldi, F., 1995. Bioaccumulation of Methylmercury and Transformation of Inorganic Mercury by Macrofungi. Environ. Sci. Technol. 29, 993–999. doi:10.1021/es00004a020

Fitzgerald, W.F., Clarkson, T.W., 1991. Mercury and monomethylmercury: present and future concerns. Environmental Health Perspectives 96, 159–166.

Fleming, E.J., Mack, E.E., Green, P.G., Nelson, D.C., 2006. Mercury Methylation from Unexpected Sources: Molybdate-Inhibited Freshwater Sediments and an Iron-Reducing Bacterium. Applied and Environmental Microbiology 72, 457–464. doi:10.1128/AEM.72.1.457-464.2006

Grigal, D.F., 2003. Mercury Sequestration in Forests and Peatlands. Journal of Environmental Quality 32, 393–405. doi:10.2134/jeq2003.3930

Guallar, E., Sanz-Gallardo, M.I., Veer, P. van't, Bode, P., Aro, A., Gómez-Aracena, J., Kark, J.D., Riemersma, R.A., Martín-Moreno, J.M., Kok, F.J., 2002. Mercury, Fish Oils, and the Risk of Myocardial Infarction. N Engl J Med 347, 1747–1754. doi:10.1056/NEJMoa020157

Hintelmann, H., Welbourn, P.M., Evans, R.D., 1995. Binding of methylmercury compounds by humic and fulvic acids. Water, Air, and Soil Pollution 80, 1031–1034. doi:10.1007/BF01189760

Hissler, C., Probst, J.-L., 2006. Impact of mercury atmospheric deposition on soils and streams in a mountainous catchment (Vosges, France) polluted by chlor-alkali industrial activity: The important trapping role of the organic matter. Science of The Total Environment 361, 163–178. doi:10.1016/j.scitotenv.2005.05.023

Holmes, C. D., D. J. Jacob, E. S. Corbitt, J. Mao, X. Yang, R. Talbot, and F. Slemr. 2010. Global Atmospheric Model for Mercury Including Oxidation by Bromine Atoms. Atmospheric Chemistry and Physics 10 (24): 12037–12057. doi:10.5194/acp-10-12037-2010.

House, A.R., Sorensen, J.P.R., Gooddy, D.C., Newell, A.J., Marchant, B., Mountford, J.O., Scarlett, P., Williams, P.J., Old, G.H., 2015. Discrete wetland groundwater discharges revealed with a three-dimensional temperature model and botanical indicators (Boxford, UK). Hydrogeology Journal 23, 775–787. doi:10.1007/s10040-015-1242-5

Iverfeldt, Å., 1991. Occurrence and turnover of atmospheric mercury over the nordic countries. Water Air & Soil Pollution 56, 251–265. doi:10.1007/BF00342275

Keller, K.L., Rapp-Giles, B.J., Semkiw, E.S., Porat, I., Brown, S.D., Wall, J.D., 2014. New model for electron flow for sulfate reduction in Desulfovibrio alaskensis G20. Applied and environmental microbiology 80, 855–868.

Kivinen, E., Pakarinen, P., 1981. Geographical Distribution of Peat Resources and Major Peatland Complex Types in the World, 3]: [Annales Academiae Scientiarum Fennicae / A. Suomalainen Tiedeakatemia.

Kronberg, R.-M., Drott, A., Jiskra, M., Wiederhold, J.G., Björn, E., Skyllberg, U., 2016. Forest harvest contribution to Boreal freshwater methyl mercury load. Global Biogeochem. Cycles 30, 2015GB005316. doi:10.1002/2015GB005316

Lantmäteriverket (2017). GSD-Höjddata, grid 2+, vector. SWEREF 99 TM. LMV. Available at: https://zeus.slu.se/get/?drop=get [2017-03-06].

Lantmäteriverket (2017). Jordarter: 1: 25 000 - 1:100 000. SWEREF 99 TM. LMV. Available at: https://zeus.slu.se/get/?drop=get [2017-03-06].

Lantmäteriverket (2017). Fastighetskartan med gränser, vector. SWEREF 99 TM. LMV. Available at: https://zeus.slu.se/get/?drop=get [2017-03-06].

Lantmäteriverket (2017). Översiktskartan, vector. SWEREF 99 TM. LMV. Available at: https://zeus.slu.se/get/?drop=get [2017-03-06].

Lantmäteriverket (2017). Terrängkartan, vector. SWEREF 99 TM. LMV. Available at: https://zeus.slu.se/get/?drop=get [2017-03-06].

Liem-Nguyen, V., Jonsson, S., Skyllberg, U., Nilsson, M.B., Andersson, A., Lundberg, E., Björn, B. 2016.Effects of Nutrient Loading and Mercury Chemical Speciation on the Formation and Degradation of Methylmercury in Estuarine Sediment. Environ. Sci. Technol. 50 (13), 6893-6990. doi:10.1021/acs.est.6b01567

Lin, C.-J., Pehkonen, S.O., 1999. The chemistry of atmospheric mercury: a review. Atmospheric Environment 33, 2067–2079. doi:10.1016/S1352-2310(98)00387-2

Lindberg, S. E., Meyers, T. P., Taylor Jr., G. E., Turner, R. R., Schroeder., W. H. 1992. Atmosphere-surface exchange of mercury in a forest: Results of modeling and gradient approaches, J. Geophys. Res., 97(D2), 2519–2528, doi:10.1029/91JD02831.

Lindberg, S.E., Stratton, W.J., 1998. Atmospheric Mercury Speciation: Concentrations and Behavior of Reactive Gaseous Mercury in Ambient Air. Environ. Sci. Technol. 32, 49–57. doi:10.1021/es970546u

Lindberg, S, Bullock, R., Ebinghaus, R., Engstrom, D., Feng, X., Fitzgerald, W., Pirrone, N., Prestbo, E., Seigneur, C., 2007. A Synthesis of Progress and Uncertainties in Attributing the Sources of Mercury in Deposition. Ambio 36, 19–32.

Lindqvist, O., Johansson, K., Bringmark, L., Timm, B., Aastrup, M., Andersson, A., Hovsenius, G., Håkanson, L., Iverfeldt, Å., Meili, M., 1991. Mercury in the Swedish environment — Recent research on causes, consequences and corrective methods. Water, Air, and Soil Pollution 55, xi-261. doi:10.1007/BF00542429

Lindsay JB. 2016. Whitebox GAT: A case study in geomorphometric analysis. Computers & Geosciences, 95: 75-84. DOI: 10.1016/j.cageo.2016.07.003

Mason, R.P., Fitzgerald, W.F., Morel, F.M.M., 1994. The biogeochemical cycling of elemental mercury: Anthropogenic influences. Geochimica et Cosmochimica Acta 58, 3191–3198. doi:10.1016/0016-7037(94)90046-9

Mason, R.P., Laporte, J.-M., Andres, S., 2000. Factors Controlling the Bioaccumulation of Mercury, Methylmercury, Arsenic, Selenium, and Cadmium by Freshwater Invertebrates and Fish. Archives of Environmental Contamination and Toxicology 38, 283–297. doi:10.1007/s002449910038

McClain, M.E., Boyer, E.W., Dent, C.L., Gergel, S.E., Grimm, N.B., Groffman, P.M., Hart, S.C., Harvey, J.W., Johnston, C.A., Mayorga, E., McDowell, W.H., Pinay, G., 2003. Biogeochemical Hot Spots and Hot Moments at the Interface of Terrestrial and Aquatic Ecosystems. Ecosystems 6, 301–312. doi:10.1007/s10021-003-0161-9

Mehrotra, A.S., Sedlak, D.L., 2005. Decrease in Net Mercury Methylation Rates Following Iron Amendment to Anoxic Wetland Sediment Slurries. Environ. Sci. Technol. 39, 2564–2570. doi:10.1021/es049096d

Minitab 17 Statistical Software (2010). [Computer software]. State College, PA: Minitab, Inc.

Morel, F.M.M., Kraepiel, A., Amyot, M., 1998. The Chemical Cycle and Bioaccumulation of Mercury. annurev.ecolsys 29, 543–566. doi:10.1146/annurev.ecolsys.29.1.543

Morris, M.A., Spencer, K.L., Belyea, L.R., Branfireun, B.A., 2014. Temporal and spatial distributions of sediment mercury in restored coastal saltmarshes. Marine Chemistry 167, 150–159. doi:10.1016/j.marchem.2014.09.010

Nagase, H., Ose, Y., Sato, T., Ishikawa, T., 1984. Mercury methylation by compounds in humic material. Science of The Total Environment 32, 147–156. doi:10.1016/0048-9697(84)90127-X

Nater, E.A., Grigal, D.F., 1992. Regional trends in mercury distribution across the Great Lakes states, north central USA. Nature 358, 139–141. doi:10.1038/358139a0

Patra, M., Sharma, A., 2000. Mercury toxicity in plants. The Botanical Review 66, 379–422. doi:10.1007/BF02868923

Qian, J., Skyllberg, U., Frech, W., Bleam, W.F., Bloom, P.R., Petit, P.E., 2002. Bonding of methyl mercury to reduced sulfur groups in soil and stream organic matter as determined by x-ray absorption spectroscopy and binding affinity studies. Geochimica et Cosmochimica Acta 66, 3873–3885. doi:10.1016/S0016-7037(02)00974-2

Qvarnström, J., French, W. 2002. Mercury species transformations during sample pretreatment of biological tissues studied by HPLC-ICP-MS. J. Anal. At. Spectrom 17, 1486-1491. doi: 10.1039/B205246F

Rea, A.W., Lindberg, S.E., Keeler, G.J., 2001. Dry deposition and foliar leaching of mercury and selected trace elements in deciduous forest throughfall. Atmospheric Environment 35, 3453–3462. doi:10.1016/S1352-2310(01)00133-9

Rudd, J.W.M., 1995. Sources of methyl mercury to freshwater ecosystems: A review. Water, Air, and Soil Pollution 80, 697–713. doi:10.1007/BF01189722

Scheuhammer, A.M., Meyer, M.W., Sandheinrich, M.B., Murray, M.W., 2007. Effects of Environmental Methylmercury on the Health of Wild Birds, Mammals, and Fish. AMBIO: A Journal of the Human Environment 36, 12–19. doi:10.1579/0044-7447(2007)36[12:EOEMOT]2.0.CO;2

Schlüter, K., 1996. Translocation of 203Hg labelled HgCl2 and CH3HgCl in an iron-humus podzol studied by radio-analytical techniques. Z. Pflanzenernaehr. Bodenk. 159, 215–226. doi:10.1002/jpln.1996.3581590218

Schoning, K., Sohlenius, G., Mikko, H., 2012. Geologisk vägledning vid ansökan om täkt för energitorv. Sveriges geologiska undersökning (SGU) - Report, 2012:12

Schuster, P.F., Shanley, J.B., Marvin-Dipasquale, M., Reddy, M.M., Aiken, G.R., Roth, D.A., Taylor, H.E., Krabbenhoft, D.P., DeWild, J.F., 2008. Mercury and Organic Carbon Dynamics During Runoff Episodes from a Northeastern USA Watershed. Water, Air, and Soil Pollution 187, 89–108. doi:10.1007/s11270-007-9500-3

Shanley, J.B., Bishop, K., 2012. Mercury Cycling in Terrestrial Watersheds, in: Mercury in the Environment, Pattern and Process. University of California Press, pp. 119–142.

Si, Y., Zou, Y., Liu, X., Si, X., Mao, J., 2015. Mercury methylation coupled to iron reduction by dissimilatory iron-reducing bacteria. Chemosphere 122, 206–212. doi:10.1016/j.chemosphere.2014.11.054

Slemr, F., Schuster, G., Seiler, W., 1985. Distribution, speciation, and budget of atmospheric mercury. Journal of Atmospheric Chemistry 3, 407–434. doi:10.1007/BF00053870

St. Louis, V.L., Rudd, J.W.M., Kelly, C.A., Beaty, K.G., Bloom, N.S., Flett, R.J., 1994. Importance of Wetlands as Sources of Methyl Mercury to Boreal Forest Ecosystems. Can. J. Fish. Aquat. Sci. 51, 1065–1076. doi:10.1139/f94-106

St. Louis, V.L., Rudd, J.W.M., Kelly, C.A., Beaty, K.G., Flett, R.J., Roulet, N.T., 1996. Production and Loss of Methylmercury and Loss of Total Mercury from Boreal Forest Catchments Containing Different Types of Wetlands. Environ. Sci. Technol. 30, 2719–2729. doi:10.1021/es950856h

St. Louis, V.L., Rudd, J.W.M., Kelly, C.A., Hall, B.D., Rolfhus, K.R., Scott, K.J., Lindberg, S.E., Dong, W., 2001. Importance of the Forest Canopy to Fluxes of Methyl Mercury and Total Mercury to Boreal Ecosystems. Environ. Sci. Technol. 35, 3089–3098. doi:10.1021/es001924p

Swartzendruber, P., Jaffe, D., 2012. Sources and Transport:, in: Mercury in the Environment, Pattern and Process. University of California Press, pp. 3–18.

Trasande, L., Landrigan, P.J., Schechter, C., 2005. Public Health and Economic Consequences of Methyl Mercury Toxicity to the Developing Brain. Environmental Health Perspectives 113, 590–596.

UNEP, 2013. Global Mercury Assessment 2013: Sources, Emissions, Releases and Environmental Transport. UNEP Chemicals Branch, Geneva, Switzerland.

Westrich, J.T., 1983. Consequences and controls of bacterial sulfate reduction in marine sediments. Yale Univ.,New Haven, CT, USA, United States.

Woodrow, K., Lindsay, J.B., Berg, A.A., 2016. Evaluating DEM conditioning techniques, elevation source data, and grid resolution for field-scale hydrological parameter extraction. Journal of Hydrology 540, 1022–1029. doi:10.1016/j.jhydrol.2016.07.018

Xia, K., Skyllberg, U.L., Bleam, W.F., Bloom, P.R., Nater, E.A., Helmke, P.A., 1999. X-ray Absorption Spectroscopic Evidence for the Complexation of Hg(II) by Reduced Sulfur in Soil Humic Substances. Environ. Sci. Technol. 33, 257–261. doi:10.1021/es980433q

Åkerblom, S., Bishop, K., Björn, E., Lambertsson, L., Eriksson, T., Nilsson, M.B., 2013. Significant interaction effects from sulfate deposition and climate on sulfur concentrations constitute major controls on methylmercury production in peatlands. Geochimica et Cosmochimica Acta 102, 1–11. doi:10.1016/j.gca.2012.10.025

Appendix

Supplementary Table 1. Major ion chemistry data from the 15 sample sites

JL1 JL2 AL1 AL2

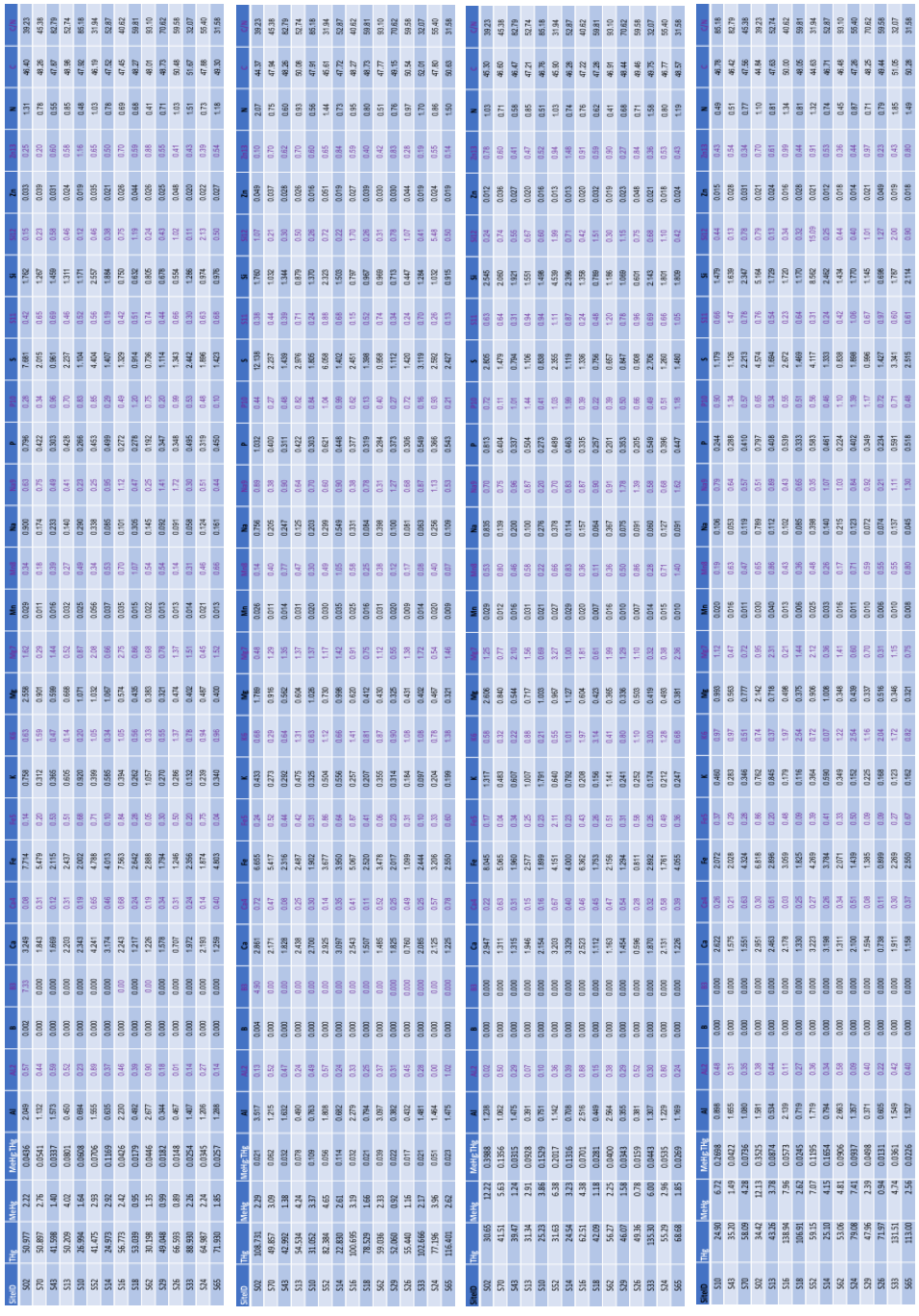

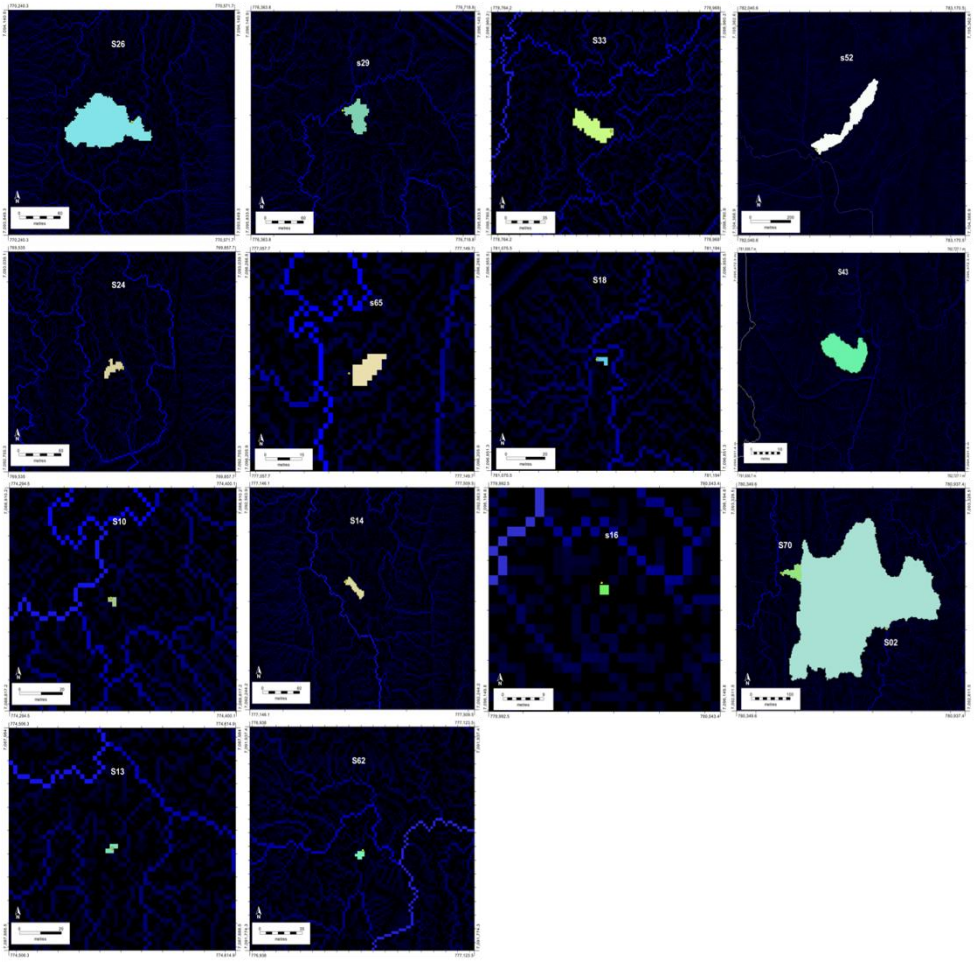

Supplementary Figure 1. 15 delineated watersheds (GSD-Höjddata, grid 2+ © Lantmäteriet)

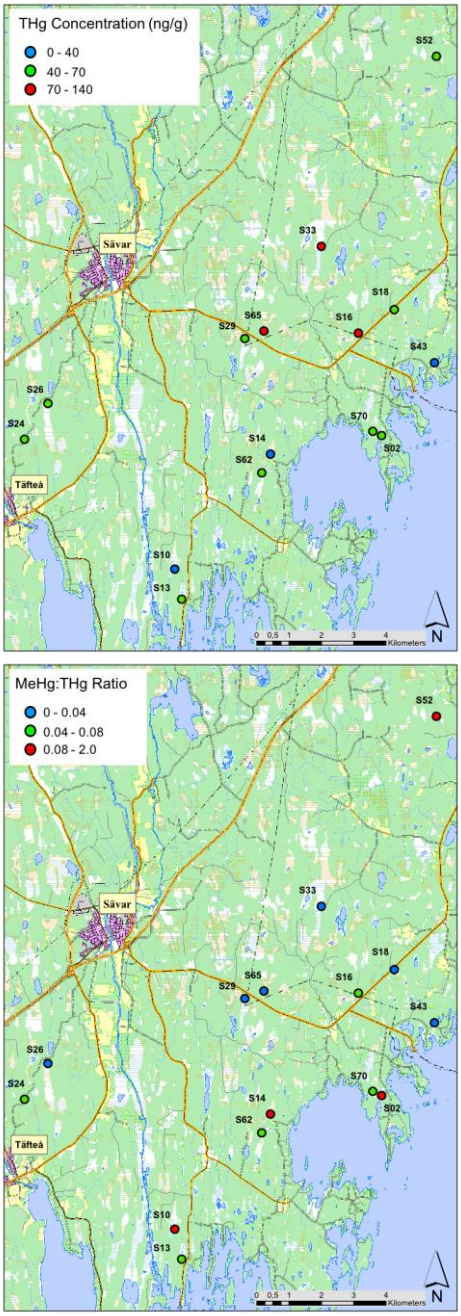

Supplementary Figure 2. Geographic distribution of top left : THg, top right: MeHg, and bottom: Me:THg of the 15 sample sites divided into low-, mid-, and high-value ranges
(see legends) (Översiktskartan, vector © Lantmäteriet)